

Collision in the interior of wormhole

Ying Zhao

Institute for Advanced Study, Princeton, NJ 08540, USA

zhaoying@ias.edu

Abstract

The Schwarzschild wormhole has been interpreted as an entangled state. If Alice and Bob fall into each of the black hole, they can meet in the interior. We interpret this meeting in terms of the quantum circuit that prepares the entangled state. Alice and Bob create growing perturbations in the circuit, and we argue that the overlap of these perturbations represents their meeting. We compare the gravity picture with circuit analysis, and identify the post-collision region as the region storing the gates that are not affected by any of the perturbations.

Contents

1	Introduction	1
2	Perturbed theomofield double and quantum circuit	3
2.1	Epidemic model	3
2.2	Quantum circuit from the point of view of Alice	4
2.3	Quantum circuit from the point of view of Bob	6
2.4	Size and interior trajectory	9
3	Collision in the interior	11
3.1	The spreading of two epidemics: overlap of two perturbations in the quantum circuit	12
3.2	Post-collision region and the number of healthy gates in the circuit	14
3.3	More detailed match of time dependence	19
4	Conclusion and Discussion	23
A	Geodesic distance	23
A.1	Geodesic distance 1	24
A.2	Geodesic distance 2	25

1 Introduction

The Schwarzschild wormhole has been interpreted as an entangled state [1]. We assume Alice and Bob share the state, each holds one half of the entangled pairs. If each of them sends in a signal at appropriate time, the two signals can meet in the interior. On the other hand there are no boundary interactions between them. This makes ER = EPR [2] a mysterious statement.

In AdS/CFT, it was argued that the bulk geometry reflects the quantum circuit preparing the boundary state [3][4][5]. In particular, in the black hole interior there is a unitary circuit preparing the state whose complexity gives the volume / action in the interior [6][7][8].

In this paper we use this quantum circuit picture to explain the “meeting” of two signals from different boundaries. When Alice and Bob send in signals, they create growing perturbations in the circuit. When both signals are sent in early enough, the two pertur-

bations will have overlap in the quantum circuit (Figure 1). We argue that this overlap represents the meeting of the two signals in the interior.

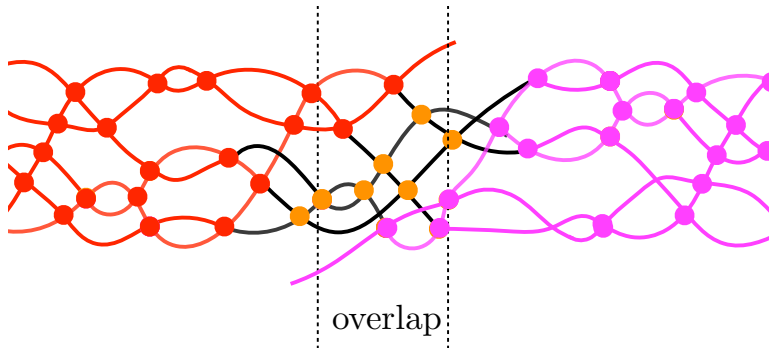


Figure 1: The two perturbations have overlap in the quantum circuit.

In [9] it was argued that different kinds of gates in the quantum circuit are stored in different parts of spacetime region. Say, Alice and Bob share thermofield double. Alice throws in a perturbation from left side at time t_w (Figure 2). We argued that from Alice's point of view, the interior geometry matches the quantum circuit in Figure 4. In particular, the interior region inside Alice's entanglement wedge stores the quantum gates that are affected by the perturbation.

In the first half of the paper we look at the same situation from Bob's point of view. We argue that we can also identify the trajectory of the infalling object in the interior close to the horizon as the perturbation in the quantum circuit (Figure 12). The closer the object is to the horizon, the larger its size is.

In the second half of the paper we consider the collision of two infalling objects in the interior of thermofield double, one sent in from the left boundary and one from the right boundary. In the corresponding quantum circuit, the two perturbations will have overlap (Figure 1). Using the epidemic model [10][11] with two epidemics coming in at different times, we estimate the number of the healthy gates in the overlap region, and show that it matches the spacetime volume of post-collision region in the gravity picture.

This paper is organized as follows. In section 2 we study the example of perturbed thermofield double from the point of view of both boundaries. We identify the trajectory of infalling object close to the horizon in the interior as corresponding to the perturbation in the quantum circuit. In section 3 we study the collision of two infalling objects in the interior, one from the left boundary and the other one from the right boundary. We show that it corresponds to the overlap between the two perturbations in the quantum circuit.

We find a detailed match between the volume of the post-collision region and the number of healthy gates from circuit analysis. In section 4 we point out unanswered questions and future directions.

2 Perturbed thermofield double and quantum circuit

Let's start from a situation where Alice and Bob share the two sides of thermofield double. Alice has the left side while Bob has the right side. Alice throws in a perturbation from the left side (Figure 2). We want to compare the geometry and quantum circuit from both the point of view of Alice and Bob.

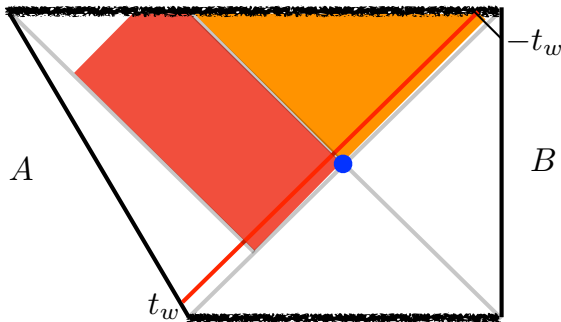


Figure 2: Thermofield double perturbed by Alice at time t_w

In Figure 2, Alice sent in a qubit from her boundary at time t_{wL} . As a result the left horizon expands. The red region in Figure 2 is the region between the new horizon after the perturbation and the old horizon without the perturbation. The RT surface stays at the blue dot.

2.1 Epidemic model

The epidemic model was introduced to describe the perturbation of a black hole [11][7]. We briefly review it here as it will play a crucial role in the rest of our discussion. We model the black hole by S qubits and we model the dynamics by a Hayden-Preskill type circuit [10]: At each time step the qubits are randomly grouped into $\frac{S}{2}$ pairs, and on each pair a randomly chosen 2-qubit gate is applied. We can characterize the effect of some small perturbation in such a system as follows. Imagine the unperturbed system contains S healthy qubits, and the perturbation is one extra qubit carrying some disease. The sick

qubit enters the system at $\tau = 0$. Any qubits who interact directly or indirectly with sick qubits will get sick. We define the size of the epidemic $s_{ep}(\tau)$ to be the number of sick qubits at time τ where τ is discrete circuit time.¹ It satisfies

$$\begin{aligned} \frac{ds_{ep}(\tau)}{d\tau} &= \frac{(S+1-s_{ep})s_{ep}}{S} \\ \frac{s_{ep}(\tau)}{S+1} &= \frac{\frac{\delta S}{S} e^{\frac{S+1}{S}\tau}}{1 + \frac{\delta S}{S} e^{\frac{S+1}{S}\tau}} = \frac{\frac{\delta S}{S} e^\tau}{1 + \frac{\delta S}{S} e^\tau} \end{aligned} \quad (2.1)$$

We used initial condition $s_{ep}(\tau = 0) = \delta S$ where δS is the number of initially infected qubits. It is proportional to the increase of thermal entropy from the perturbation. Later we will adjust the prefactor to make a better match with the gravity picture.

Assume Alice and Bob share thermofield double and Alice applies the perturbation. At each time step from $\tau - \Delta\tau$ to τ , S gates are applied on Alice's side.² Among them, $s_{ep}(\tau)$ gates involve the extra qubit and cannot be undone by Bob. The remaining $S - s_{ep}(\tau)$ gates can be undone by Alice as well as Bob.

2.2 Quantum circuit from the point of view of Alice

We first look at the quantum circuit without perturbations. We represent the black hole by S Bell pairs. As the left (right) boundary time increases, the circuit grows toward left (right) (Figure 3(a)). The wormhole also grows (Figure 3(b)).

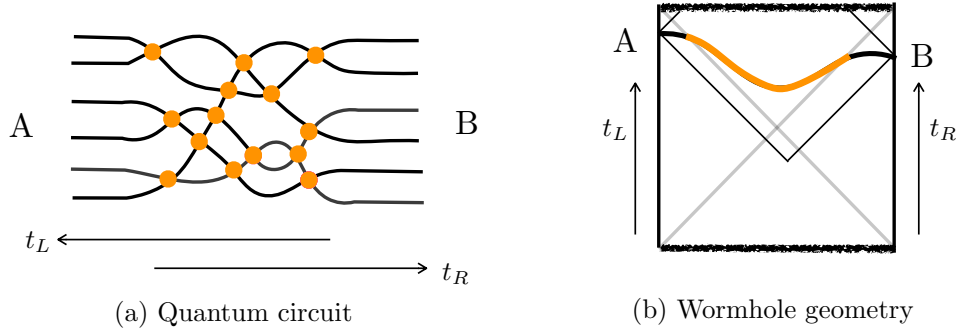


Figure 3: The wormhole grows as the circuit grows.

Now Alice sends in some perturbation from left boundary at time t_w . In the quantum

¹Later we will identify the circuit time and Schwarzschild time: $d\tau = \frac{2\pi}{\beta} dt$.

²We count each 2-qubit gate as 2 gates.

circuit picture, we model Alice's perturbation by throwing in an extra qubit. Here is the reason: Alice's perturbation cannot be undone by Bob, so it changes Alice's density matrix. In particular, Alice's density matrix will no longer be exactly thermal, and its thermal entropy will be larger than fine-grained entropy. We use this extra qubit to represent the increase of thermal entropy.

In [9] it was argued that the gates in the quantum circuit that can be undone by both Alice and Bob are stored in the shared entanglement region (orange region in Figure 4), while the gates that can be undone by Alice but not by Bob are stored in Alice's entanglement wedge (red region in Figure 4). The spacetime volumes in these regions were compared with the epidemic model of quantum circuit. The exact quantity to look at doesn't matter. One can instead look at the geodesic distance between the two boundaries.

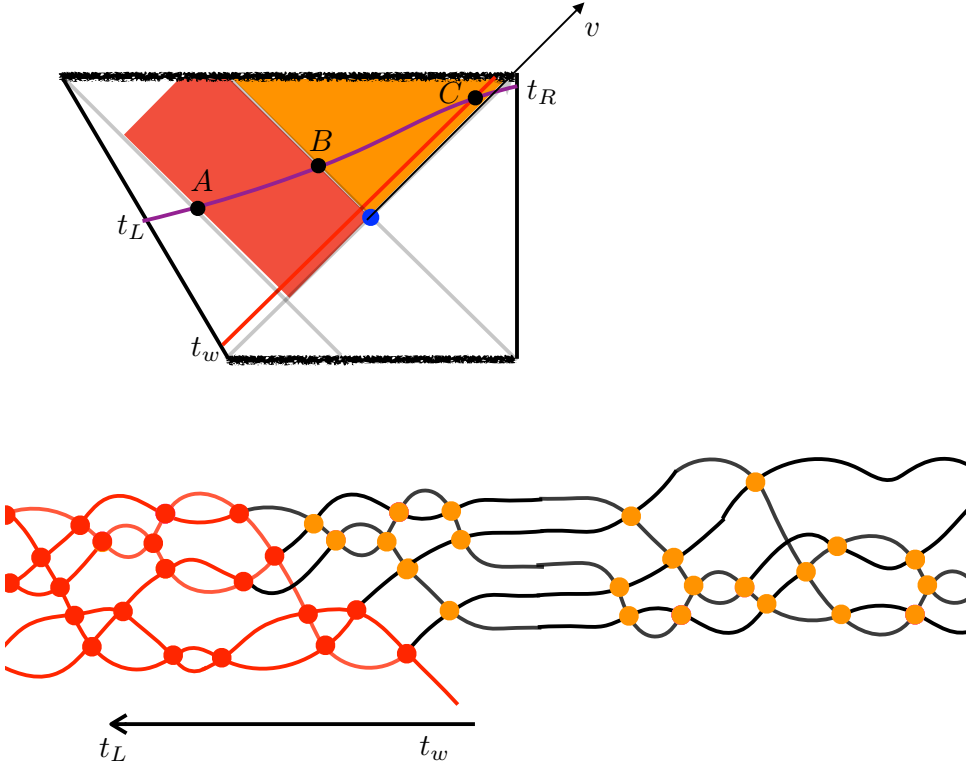


Figure 4: Penrose diagram and quantum circuit of perturbed thermofield double

We fix some very large right time $t_R \rightarrow \infty$ and vary the left time t_L . Instead of looking at the entire geodesic between the two boundaries, we focus on the part of the geodesic contained in the orange region as well as the red region in Figure 4. We want to say the the growth of the orange region (geodesic BC) corresponds to the growth of the orange gates

in the circuit in Figure 4 (the gates that can be undone by both Alice and Bob), while the growth of the red region (geodesic AB) corresponds to the growth of the red gates (the gates that can be undone by Alice but not by Bob). In BTZ black hole geometry, one can show that (appendix A.1)

$$\frac{d}{dt_L} \left(\frac{d_{AB}}{l} \right) = \frac{2\pi}{\beta} \frac{e^{\frac{2\pi}{\beta}(t_L - t_w - t_*)}}{1 + e^{\frac{2\pi}{\beta}(t_L - t_w - t_*)}} = \frac{2\pi}{\beta} \left(\frac{s_{ep}[\frac{2\pi}{\beta}(t_L - t_w)]}{S} \right)$$

$$\frac{d}{dt_L} \left(\frac{d_{BC}}{l} \right) = \frac{2\pi}{\beta} \frac{1}{1 + e^{\frac{2\pi}{\beta}(t_L - t_w - t_*)}} = \frac{2\pi}{\beta} \left(1 - \frac{s_{ep}[\frac{2\pi}{\beta}(t_L - t_w)]}{S} \right)$$

where $s_{ep}(\tau)$ is the size function in epidemic model as in (2.1). The above geodesic length calculation shows perfect match with the epidemic model. The fact that the match is perfect may be an artifact of the special geometry of BTZ as well as its geodesic distance. The lesson is that the growth of certain spacetime regions shows the same features of time dependence as the growth of certain kinds of gates in the quantum circuit, like exponential growth, saturation after scrambling time, etc.

2.3 Quantum circuit from the point of view of Bob

Let's first consider the situation when there is no shockwave and Alice and Bob share standard thermofield double. We put left time at $t_L = +\infty$. As Bob decreases the right time t_R , he will undo the gates stored in the future interior at a steady rate (Figure 5).

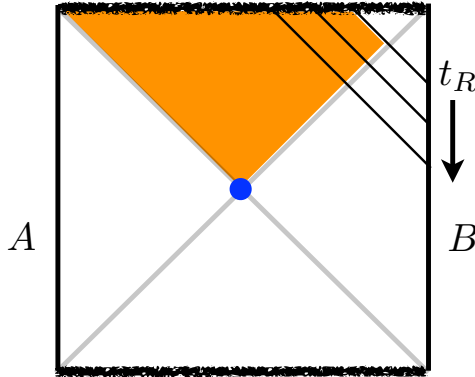


Figure 5: As Bob decreases the right time, he will undo the gates stored in the future interior (orange region) at a steady rate.

Now we consider the situation where Alice sent in a perturbation from her side. We

look at the quantum circuit in Figure 4 from the point of view of Bob. What do we expect? Bob should be able to undo the orange gates but Bob cannot undo the red gates. The existence of those red gates will affect the rate at which Bob can undo the orange gates. We again look at the time dependence of geodesic inside the future entanglement region (orange region), but this time we fix the left time at $+\infty$ and vary the right time (Figure 27). Here is its time dependence we found in BTZ background (appendix A.2).

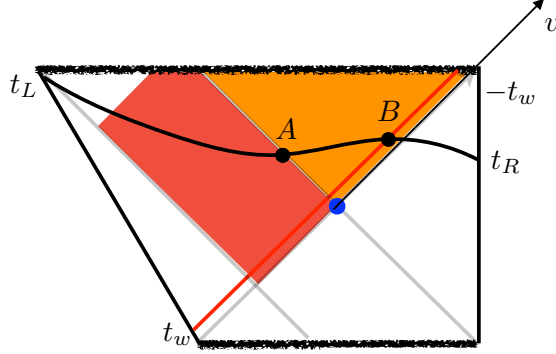


Figure 6: We fix the left time at future infinity and vary the right time.

$$\begin{aligned} \frac{d_{AB}}{l} &= \frac{2\pi}{\beta}(t_R + t_w + t_*) + \log\left(1 + \alpha e^{-\frac{2\pi}{\beta}t_R}\right) \\ \frac{d}{dt_R} \frac{d_{AB}}{l} &= \frac{2\pi}{\beta} \left[1 - \frac{e^{\frac{2\pi}{\beta}(-t_w - t_* - t_R)}}{1 + e^{\frac{2\pi}{\beta}(-t_w - t_* - t_R)}} \right] = \frac{2\pi}{\beta} \left(1 - \frac{s_{ep}\left[\frac{2\pi}{\beta}(-t_w - t_R)\right]}{S} \right) \end{aligned} \quad (2.2)$$

So far we only looked at the time dependence of the length of geodesic in the future interior region. If we take the point of view that the bulk dual to a boundary state is the entire Wheeler-DeWitt (WDW) patch, we can say more. Imagine that during the time t_R and $t_R - \Delta t$, $S\Delta t$ gates are applied in the right CFT. Among them, $S\Delta t(1 - \frac{s_{ep}}{S})$ gates are cancelled by the gates stored in the future interior. Then what happens to the remaining $s_{ep}\Delta t$ gates? They are stored in the past interior. See Figure 7³.

³I thank Juan Maldacena for correcting me on this.

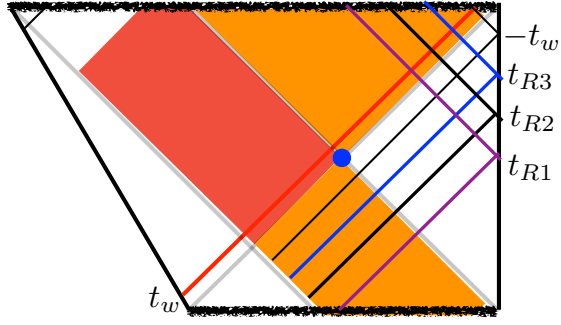


Figure 7: During each time step as we decrease the right time, $S - s_{ep}$ gates are cancelled by the gates in the future interior. The remaining s_{ep} gates are stored in the past interior.

Here are comparisons of the quantum circuit and WDW patch at different times. With fixed t_L large, Figure 8 shows the quantum circuit and WDW patch in Penrose diagram at $t_R > -t_w$.

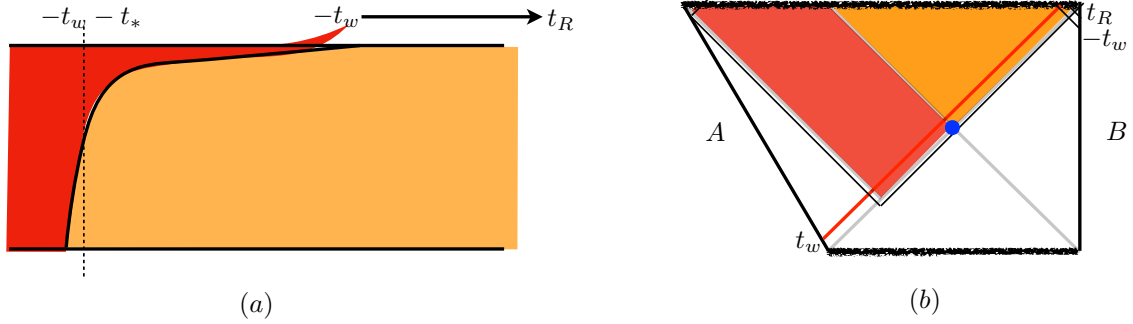


Figure 8: Quantum circuit and WDW patch at $t_R > -t_w$.

Now Bob decrease the right time t_R . He can undo the orange gates in Figure 8(a), but he cannot undo the red gates. Instead, he will create a fold on top of the red gates (Figure 9(a)).⁴ This fold is stored in the past interior (Figure 9(b)).

⁴This was pointed out to me by Juan Maldacena.

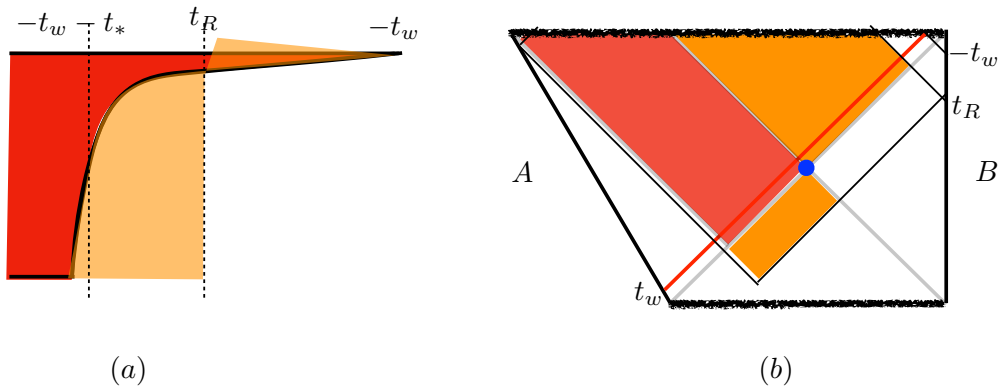


Figure 9: Quantum circuit and WDW patch at $-t_w - t_* < t_R < -t_w$.

If Bob further decreases the right time until $t_R < -t_w - t_*$, all the orange gates in Figure 8(a) have been undone. The gates in the extra fold are stored in the past interior (Figure 10).

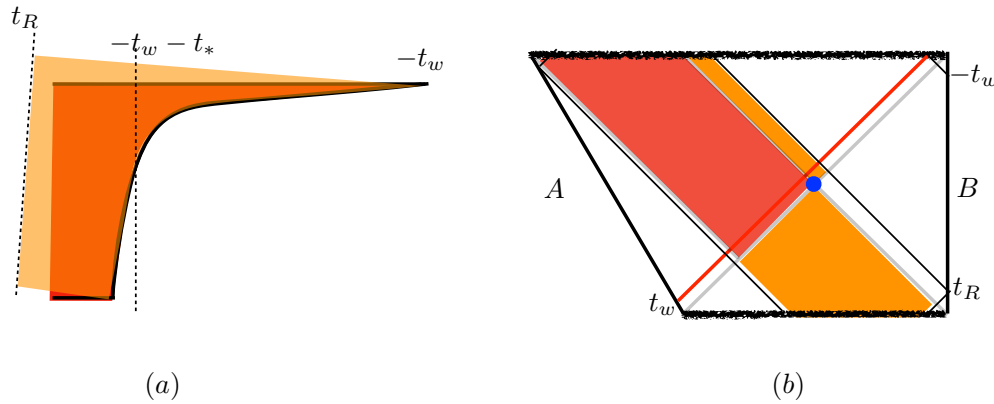


Figure 10: Quantum circuit and WDW patch at $t_R < -t_w - t_*$.

2.4 Size and interior trajectory

We see that since Bob cannot undo the red gates in the quantum circuit in Figure 4, the complexity has non-trivial time dependence as he changes the right time.

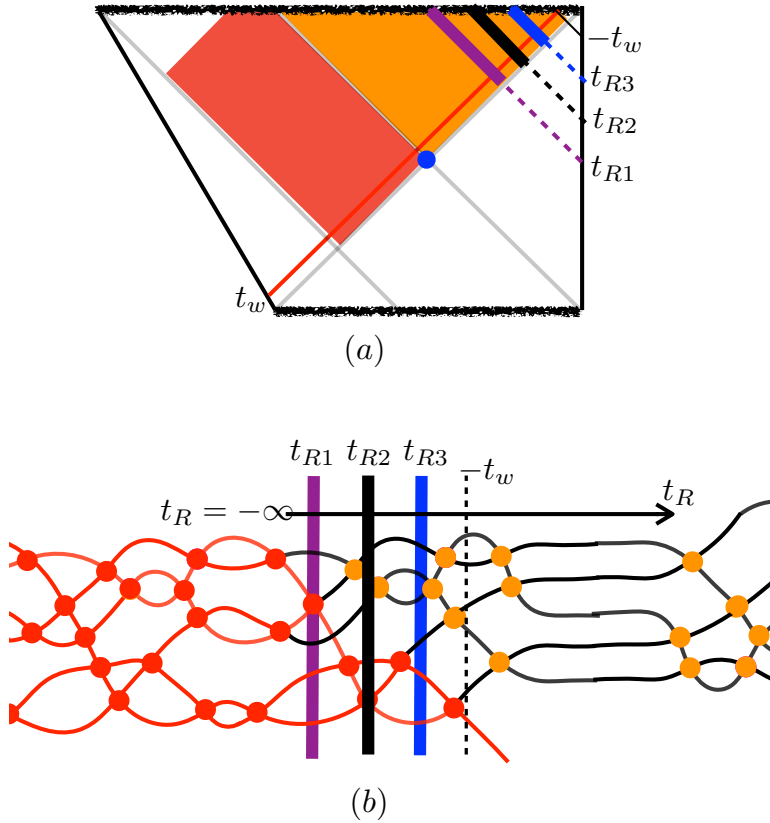


Figure 11: When Bob decreases the right time, he is scanning through the quantum circuit from the right to the left.

The time dependence of the geodesic length in (2.2) shows that when Bob decreases the right time, he is scanning through the quantum circuit from the right to the left (Figure 11). He will encounter the perturbation at $t_R = -t_w$. In Figure 11(a) we draw three sections in the Penrose diagram, which correspond to three sections in the quantum circuit of the same color in Figure 11(b). In this sense one can identify the part of the shockwave trajectory in the interior near the horizon as the perturbation in the quantum circuit (Figure 12). The closer the object is to the horizon, the larger its size is.

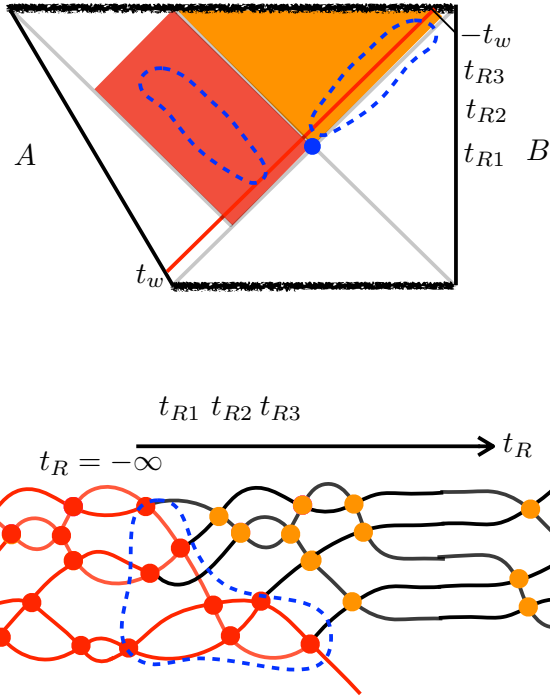


Figure 12: We can identify the part of the interior shockwave trajectory near the horizon as the perturbation in the quantum circuit.

If we look at the Penrose diagram in Figure 12, we see that both the red region inside Alice’s entanglement wedge and the trajectory of the infalling object inside the orange region have to do with the perturbation in the quantum circuit. We circled them out in blue dashed circles. We see complementarity at play here [12].

3 Collision in the interior

It’s a mysterious feature in ER = EPR that infalling objects from the two boundaries can meet in the shared interior (Figure 13), as there are no interactions between them in the boundary theory. Here, we give a quantum circuit interpretation of this phenomenon.

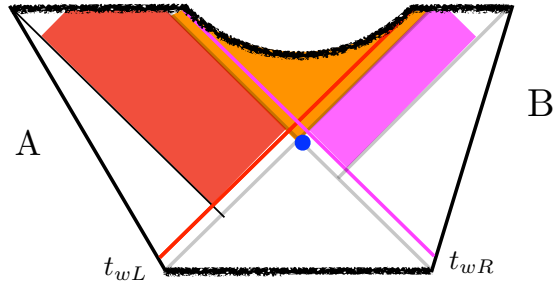


Figure 13: Infalling objects from the two boundaries can meet in the interior.

3.1 The spreading of two epidemics: overlap of two perturbations in the quantum circuit

Let's start from thermofield double shared between Alice and Bob. We model the quantum circuit by S maximally entangled Bell pairs. Now Alice throws in a qubit from the left boundary at time t_{wL} , and Bob throws in a qubit from the right boundary at time t_{wR} . We first assume $t_{wL} > 0$ and $t_{wR} > 0$. In the corresponding quantum circuit, there will be no overlaps between the two perturbations (Figure 14).

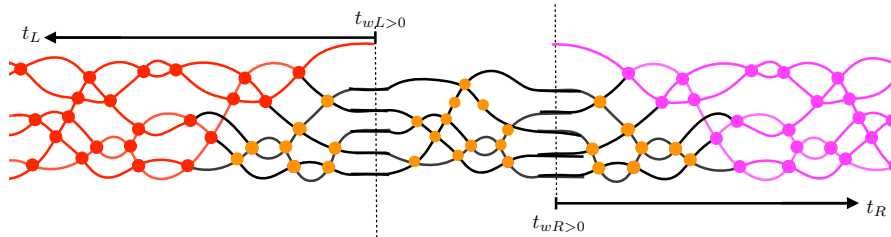


Figure 14: The two perturbations do not overlap in the quantum circuit.

Correspondingly, the two perturbations do not collide in the interior (Figure 15).

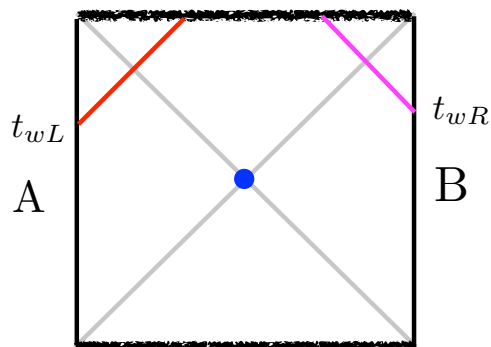


Figure 15: The two infalling objects do not meet in the interior.

Next we assume $t_{wL} < 0$ and $t_{wR} < 0$. The two perturbations will have overlap in the quantum circuit (Figure 16).

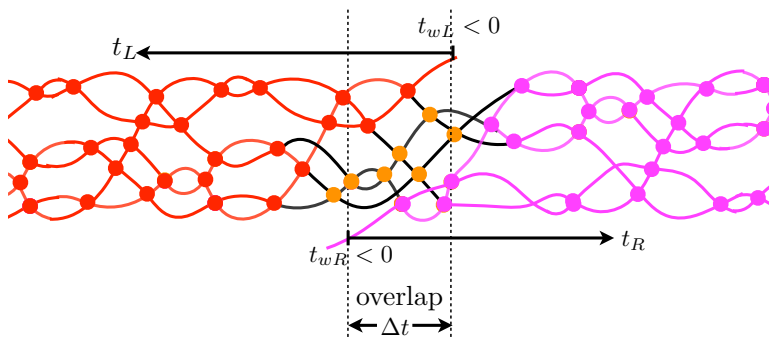


Figure 16: The two perturbations have overlap in the quantum circuit.

Correspondingly, the two perturbations will collide in the interior (Figure 13).

Imagine we have a quantum circuit made of orange gates that can be undone from both sides. We call these orange gates healthy gates. Now a red epidemic comes in at time $-t_{wL} > 0$ ⁵ and propagates toward the left of the circuit. Also, a purple epidemic comes in at time $t_{wR} < 0$ and propagates toward the right (Figure 16). In the next section, we will estimate the number of healthy gates in the overlapping region of the circuit and compare it with the volume of the post-collision region in gravity picture.

⁵We identify the circuit time with the right time t_R , and with minus the left time $-t_L$.

3.2 Post-collision region and the number of healthy gates in the circuit

We look at the quantum circuit model with two overlapping epidemics. Let $\Delta t \equiv -t_{wL} - t_{wR}$ be the overlapping time of the two epidemics (Figure 16).

We estimate the number of healthy gates in the overlap region of the quantum circuit. In Figure 17, the probability of being healthy from the red epidemic is $(1 - \frac{s_{ep}^{red}}{S}) = \frac{1}{1 + \frac{\delta S_1}{S} e^{\frac{2\pi}{\beta}(-t_{wL}-t)}}$. The probability of being healthy from the purple epidemic is $(1 - \frac{s_{ep}^{purple}}{S}) = \frac{1}{1 + \frac{\delta S_2}{S} e^{\frac{2\pi}{\beta}(t-t_{wR})}}$. The probability of being healthy from both epidemics in the overlap region is the product of these two.

1. Early time: $\frac{\beta}{2\pi} \ll \Delta t \ll t_*$

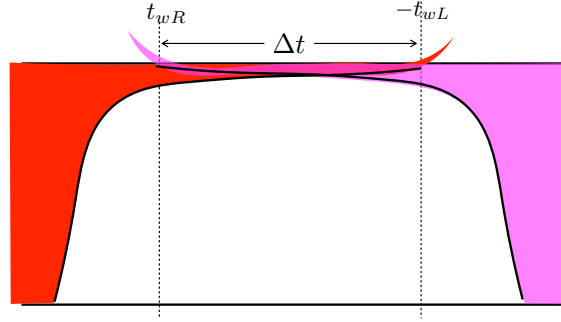


Figure 17: $\frac{\beta}{2\pi} \ll \Delta t \ll t_*$. The red region represents the gates contaminated by the red epidemic. The purple region represents the gates contaminated by the purple epidemic. The white region represents the healthy gates.

The number of healthy gates in the overlap region is given by

$$\begin{aligned} \frac{N_{\text{healthy}}}{S} &= \int_{t_{wR}}^{-t_{wL}} \frac{2\pi}{\beta} dt \left(\frac{1}{1 + \frac{\delta S_1}{S} e^{\frac{2\pi}{\beta}(-t_{wL}-t)}} \right) \left(\frac{1}{1 + \frac{\delta S_2}{S} e^{\frac{2\pi}{\beta}(t-t_{wR})}} \right) \\ &= \frac{2\pi}{\beta} \Delta t - \frac{\delta S_1 + \delta S_2}{S} e^{\frac{2\pi}{\beta} \Delta t} + \mathcal{O} \left(\left(\frac{1}{K} e^{\frac{2\pi}{\beta} \Delta t} \right)^2 \right) \end{aligned} \quad (3.3)$$

Now we look at the Penrose diagram. The collision happens at radius $r_c = r_h \tanh\left(\frac{\pi}{\beta} \Delta t\right)$. In the post collision region, a larger black hole forms. In BTZ geometry, the new

horizon radius \tilde{r}_h is given by [13][14]⁶

$$\frac{\tilde{r}_h^2}{r_h^2} = 1 + \frac{2\delta S_1}{S} + \frac{2\delta S_2}{S} + \frac{4\delta S_1\delta S_2}{S^2} \cosh^2\left(\frac{\pi}{\beta}\Delta t\right)$$

The spacetime volume in the post collision region is given by

$$V = 2\pi\tilde{r}_h l^2 \left(\frac{1}{2} \log \frac{\tilde{r}_h + r_c}{\tilde{r}_h - r_c} - \frac{r_c}{\tilde{r}_h} \right)$$

In the early regime where $\frac{\beta}{2\pi} \ll \Delta t \ll t_*$, we have

$$\begin{aligned} \frac{V}{\pi\tilde{r}_h l^2} &= \log \frac{1 + \frac{\delta S_1}{S} + \frac{\delta S_2}{S} + \tanh\left(\frac{\pi}{\beta}\Delta t\right)}{1 + \frac{\delta S_1}{S} + \frac{\delta S_2}{S} - \tanh\left(\frac{\pi}{\beta}\Delta t\right)} - 2 \frac{\tanh\left(\frac{\pi}{\beta}\Delta t\right)}{1 + \frac{\delta S_1 + \delta S_2}{S}} \\ &\approx \frac{2\pi}{\beta}\Delta t - \frac{\delta S_1 + \delta S_2}{S} \sinh\left(\frac{2\pi}{\beta}\Delta t\right) \\ \frac{V}{\pi r_h l^2} &\approx \frac{2\pi}{\beta}\Delta t - \frac{\delta S_1 + \delta S_2}{2S} e^{\frac{2\pi}{\beta}\Delta t} \end{aligned} \quad (3.4)$$

(3.3) and (3.4) agree up to a shift of Δt .

In this case, we can also look at the total number of healthy gates (the entire white region in Figure 17) and compare it with the volume of the entire future interior region shared between the the two sides (orange region in Figure 18).

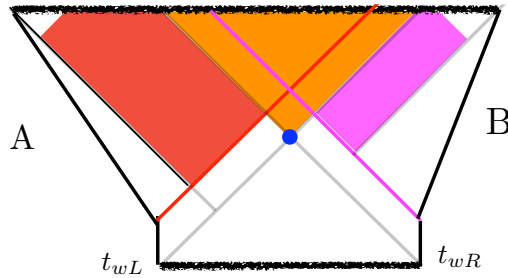


Figure 18: At early time, the entire shared future interior region (orange region) is larger than the post-collision region.

⁶This result depends on spherical symmetry as well as thin wall approximation.

The total number of healthy gates is given by

$$\begin{aligned} \frac{N_{\text{healthy}}^{\text{total}}}{S} &= \int_{-\infty}^{+\infty} \frac{2\pi}{\beta} dt \left(\frac{1}{1 + \frac{\delta S_1}{S} e^{\frac{2\pi}{\beta}(-t_{wL}-t)}} \right) \left(\frac{1}{1 + \frac{\delta S_2}{S} e^{\frac{2\pi}{\beta}(t-t_{wR})}} \right) \\ &\approx \frac{2\pi}{\beta} (2t_* - \Delta t) \end{aligned} \quad (3.5)$$

On the other hand, the spacetime volume in the entire shared future interior region (orange region in Figure 18) is given by

$$\frac{V}{\pi r_h l^2} \approx \frac{2\pi}{\beta} (2t_* - \Delta t) \quad (3.6)$$

(3.6) agrees with (3.5).

2. Intermediate time: $t_* \ll \Delta t \ll 2t_*$

Next, we look at the intermediate regime when $t_* \ll -t_{wL} - t_{wR} \ll 2t_*$. Here is the circuit picture.

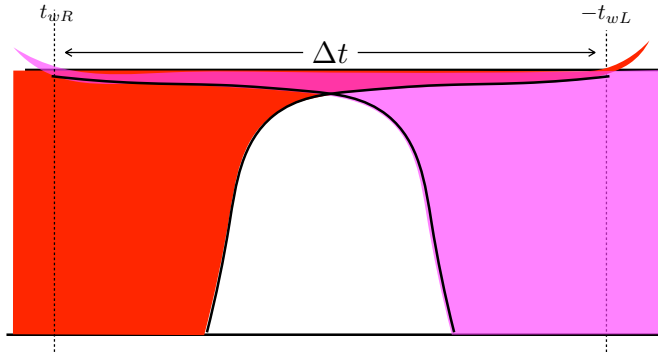


Figure 19: $t_* \ll \Delta t \ll 2t_*$. The number of healthy gates starts to decrease as a function of Δt .

The number of healthy gates in the overlap region is given by

$$\begin{aligned} \frac{N_{\text{healthy}}}{S} &= \int_{t_{wR}}^{-t_{wL}} \frac{2\pi}{\beta} dt \left(\frac{1}{1 + \frac{\delta S_1}{S} e^{\frac{2\pi}{\beta}(-t_{wL}-t)}} \right) \left(\frac{1}{1 + \frac{\delta S_2}{S} e^{\frac{2\pi}{\beta}(t-t_{wR})}} \right) \\ &\approx \frac{2\pi}{\beta} (2t_* - \Delta t) \left(1 + \frac{\delta S_1 \delta S_2 e^{\Delta t}}{S^2} \right) \end{aligned} \quad (3.7)$$

We look at the spacetime volume in the intermediate regime.

$$\begin{aligned}
\frac{V}{\pi \tilde{r}_h l^2} &= \log \frac{2 + \frac{2\delta S_1 \delta S_2}{S^2} \cosh^2\left(\frac{\pi}{\beta} \Delta t\right)}{\frac{2\delta_1 \delta_2}{S^2} \cosh^2\left(\frac{\pi}{\beta} \Delta t\right)} - \frac{2}{1 + \frac{2\delta S_1 \delta S_2}{S^2} \cosh^2 \frac{\pi}{\beta} \Delta t} \\
&\approx \frac{2\pi}{\beta} (2t_* - \Delta t) \\
\frac{V}{\pi r_h l^2} &\approx \frac{2\pi}{\beta} (2t_* - \Delta t) \left(1 + \frac{\delta S_1 \delta S_2}{2S^2} e^{\frac{2\pi}{\beta} \Delta t}\right)
\end{aligned} \tag{3.8}$$

We again see that (3.7) and (3.8) agree up to a shift in Δt .

3. Late time: $\Delta t \gg 2t_*$

Now we look at the third regime where $\Delta t \gg 2t_*$. From the quantum circuit picture, we no longer expect there to be healthy gates.

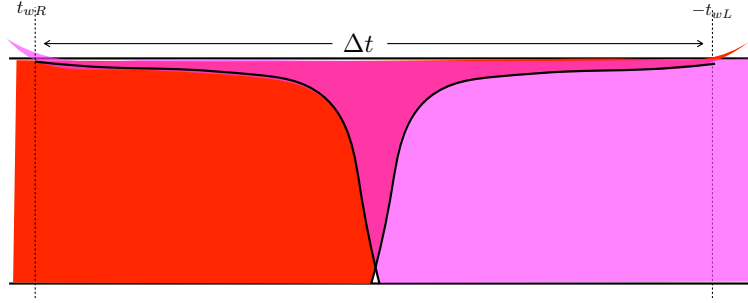


Figure 20: $\Delta t \gg 2t_*$. There are almost no healthy gates.

The epidemic model gives the number of healthy gates

$$\begin{aligned}
\frac{N_{\text{healthy}}}{S} &= \int_{t_{wR}}^{-t_{wL}} \frac{2\pi}{\beta} dt \left(\frac{1}{1 + \frac{\delta S_1}{S} e^{\frac{2\pi}{\beta} (-t_{wL} - t)}} \right) \left(\frac{1}{1 + \frac{\delta S_2}{S} e^{\frac{2\pi}{\beta} (t - t_{wR})}} \right) \\
&\approx e^{-\frac{2\pi}{\beta} (\Delta t - 2t_*)} (\Delta t - 2t_*)
\end{aligned}$$

On the gravity side, the post collision region is exponentially small and exponentially

close to the singularity. We have

$$\begin{aligned} \frac{V}{\pi \tilde{r}_h l^2} &= \log \frac{e^{\frac{\pi}{\beta}(\Delta t - 2t_*)} + 1}{e^{\frac{\pi}{\beta}(\Delta t - 2t_*)} - 1} - \frac{2}{e^{\frac{\pi}{\beta}(\Delta t - 2t_*)}} \\ &\approx \frac{2}{3} e^{-\frac{3\pi}{\beta}(\Delta t - 2t_*)} \\ \frac{V}{\pi r_h l^2} &\approx \frac{2}{3} e^{-\frac{2\pi}{\beta}(\Delta t - t_*)} \end{aligned}$$

In this case, the epidemic model and the spacetime volume calculation don't exactly match, but they both decrease exponentially in $\frac{2\pi}{\beta}(\Delta t - 2t_*)$.

Here is a plot of the volume of the post collision region and the number of healthy gates as a function of Δt in the entire range: $0 < \Delta t < 3t_*$. We took $\frac{2\pi}{\beta}t_* = 36$.

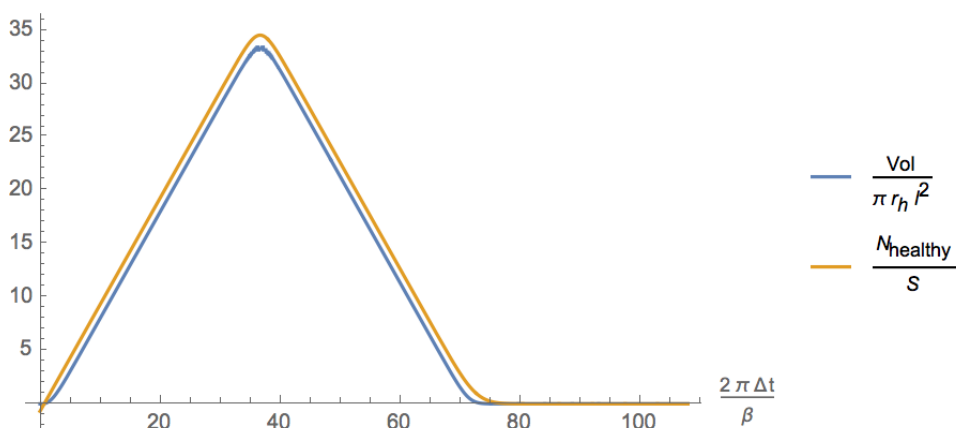


Figure 21: The volume of the post collision region and the number of healthy gates as a function of Δt . We take $\frac{2\pi}{\beta}t_* = 36$.

They differ by an order one constant, corresponding to the gates in one thermal time. One can instead look at their derivative with respect to Δt :

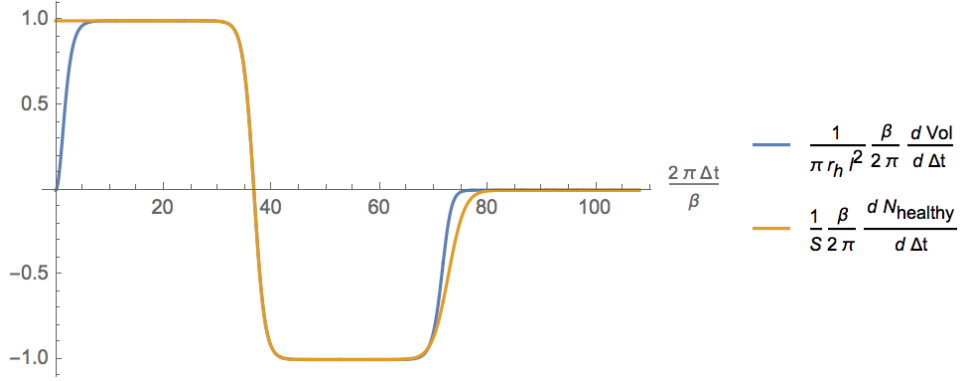


Figure 22: The time derivative of volume of the post collision region and the number of healthy gates as a function of Δt . We take $\frac{2\pi}{\beta}t_* = 36$.

We see good match except for at Δt of order thermal time or Δt close to $2t_*$.

We can also estimate the number of gates contaminated by both epidemics. The ratio of the number of such gates with the number of healthy gates is proportional to the collision energy. This is a curious fact but we don't have an interpretation.

3.3 More detailed match of time dependence

Based on the assumption that the collision in the interior corresponds to the overlap of perturbations in the quantum circuit, we've seen there is a good match between the number of healthy gates in the circuit model and the spacetime volume of the post-collision region. In fact, we can do a more-detailed match.

We can vary the right time, and see how the spacetime volume in the post-collision region inside the future interior depends on the right time.

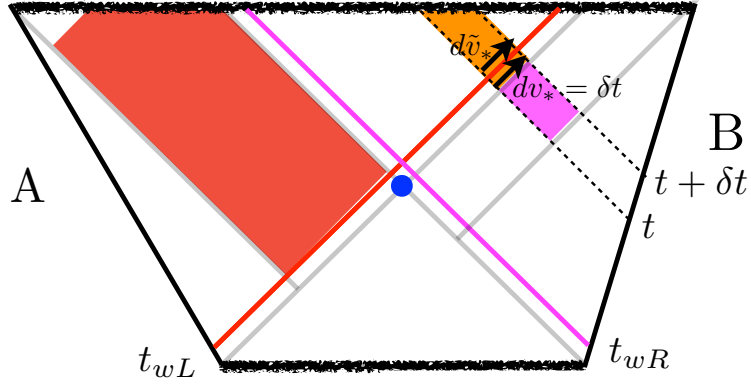


Figure 23: The dependence of the volume of post collision region on the right time.

We write BTZ metric as $ds^2 = -f(r)dv_*^2 + 2drdv_* + r^2d\phi^2$. In the post collision region, we replace $f(r)$ by $\tilde{f}(r)$. In Figure 23, we have

$$dv_* = \frac{2}{f(r)}dr, \quad \frac{d\tilde{v}_*}{dv_*} = \frac{f(r)}{\tilde{f}(r)}$$

$$\frac{d\text{Vol}_{\text{orange}}}{dt} = \int_0^{r(t)} dr r d\phi \frac{d\tilde{v}_*}{dv_*} = \pi r(t)^2 \frac{r_h^2 - r(t)^2}{\tilde{r}_h^2 - r(t)^2}$$

$$\begin{aligned}
\frac{1}{\pi r_h^2} \frac{d\text{Vol}_{\text{orange}}}{dt} &= \left(\frac{1 - \frac{\delta S_2}{2S} e^{-\frac{2\pi}{\beta} t_{wR}} e^{\frac{2\pi}{\beta} t}}{1 + \frac{\delta S_2}{2S} e^{-\frac{2\pi}{\beta} t_{wR}} e^{\frac{2\pi}{\beta} t}} \right)^2 \left(\frac{1 - \left(\frac{1 - \frac{\delta S_2}{2S} e^{-\frac{2\pi}{\beta} t_{wR}} e^{\frac{2\pi}{\beta} t}}{1 + \frac{\delta S_2}{2S} e^{-\frac{2\pi}{\beta} t_{wR}} e^{\frac{2\pi}{\beta} t}} \right)^2}{1 + \frac{4\delta S_1 \delta S_2}{S^2} \cosh^2 \frac{\pi}{\beta} (-t_{wL} - t_{wR}) - \left(\frac{1 - \frac{\delta S_2}{2S} e^{-\frac{2\pi}{\beta} t_{wR}} e^{\frac{2\pi}{\beta} t}}{1 + \frac{\delta S_2}{2S} e^{-\frac{2\pi}{\beta} t_{wR}} e^{\frac{2\pi}{\beta} t}} \right)^2} \right) \\
&= \tanh^2 \left(\frac{\pi}{\beta} (t - t_{wR} - t_*) \right) \left(\frac{1}{1 + \cosh^2 \left(\frac{\pi}{\beta} (t_{wR} + t_* - t) \right) \exp \left(\left(\frac{2\pi}{\beta} (-t_{wL} - t_{wR} - 2t_*) \right) \right)} \right) \\
&= \left(\frac{1}{1 + \frac{2\delta S_2}{S} e^{\frac{2\pi}{\beta} (t - t_{wR})} + \mathcal{O} \left(\left(\frac{\delta S_2}{S} e^{\frac{2\pi}{\beta} (t - t_{wR})} \right)^2 \right)} \right) \\
&\quad \left(\frac{1}{1 + \frac{\delta S_1}{2S} \exp \left(\frac{2\pi}{\beta} (-t_{wL} - t) \right) + \frac{1}{2} \exp \left(\frac{2\pi}{\beta} (\Delta t - 2t_*) \right) + \mathcal{O} \left(\left(\frac{1}{S} e^{\frac{2\pi}{\beta} (t - t_{wR})} \right)^2 \right)} \right)
\end{aligned} \tag{3.9}$$

We want to compare this with the circuit answer:

$$\left(1 - \frac{s_{ep} \left[\frac{2\pi}{\beta} (t - t_{wR}) \right]}{\text{size}_{\text{max}}} \right) \left(1 - \frac{s_{ep} \left[\frac{2\pi}{\beta} (-t_{wL} - t) \right]}{\text{size}_{\text{max}}} \right) = \left(\frac{1}{1 + \frac{\delta S_1}{S} e^{t - t_{wR}}} \right) \left(\frac{1}{1 + \frac{\delta S_2}{S} e^{-t_{wL} - t}} \right) \tag{3.10}$$

We see that these two answers have good match with a shift of t as long as $\frac{1}{K} e^{t - t_{wR}} < 1$. This explains the match between the number of healthy gates and the volume of post-collision region. The total volume of post collision region is the integral of (3.9), while the number of healthy gates is the integral of (3.10).

Here is a plot of (3.9) and (3.10), with $\frac{2\pi}{\beta} (t_{wR} + t_*) = 40$, $\frac{2\pi}{\beta} (-t_{wL} - t_*) = 0$.

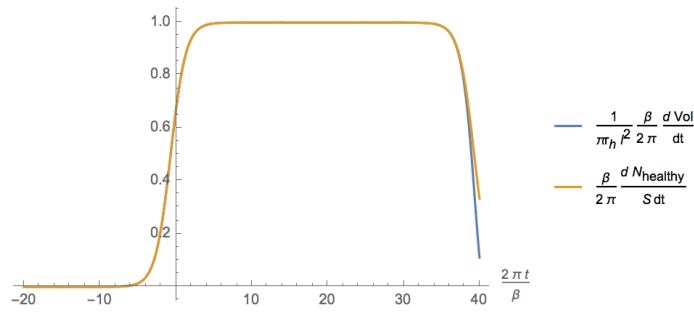


Figure 24: Plot of (3.9) and (3.10). We take $\frac{2\pi}{\beta}(t_{wR} + t_*) = 40$, $\frac{2\pi}{\beta}(-t_{wL} - t_*) = 0$.

What this computation shows is that, if we focus on how the volume of the post-collision region changes while we increase the right time t_R (Figure 25(a)), it behaves as if we are scanning through the circuit from left to the right (Figure 25(b)).

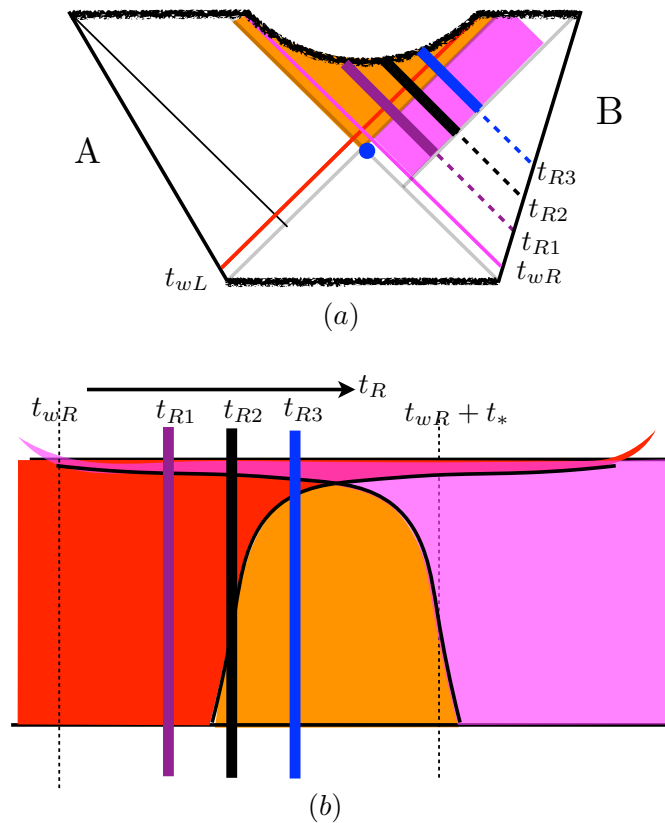


Figure 25: When we increase the right time and see how the volume of the post-collision region changes, it behaves as if we are scanning through the circuit from the left to the right.

4 Conclusion and Discussion

We compared quantum circuit picture with interior geometry, and concluded that the trajectory of an infalling object in the interior near the horizon corresponds to the perturbation in the quantum circuit.

We also explored the idea that collision in the interior of thermofield double reflects the overlap of perturbations in the quantum circuit, and found good match between the number of healthy gates in the circuit model and the spacetime volume of the post collision region.

There are many unanswered questions. In this paper we only considered neutral black holes. How do charged black holes fit into the story? For charged black hole, two perturbations falling in from two boundaries at t_{wL} and t_{wR} will collide even when both times are large positive.

We argued that the collision of objects in the interior corresponds to the overlaps of two perturbations in the circuit. But how to diagnose if the two perturbations overlap or not? The two operators W_L and W_R always commute.

Our story is only sensitive to the portion of the trajectory of infalling object when it is close to the horizon. We didn't say anything about the singularity. From the picture of neutral black holes, one tends to say that at the singularity the perturbation has smallest size and becomes simple, but this picture doesn't work for charged black holes.

Acknowledgements

I thank Ahmed Almheiri, Yiming Chen, Adam Levine, Henry Lin, Leonard Susskind, Edward Witten for helpful discussions. I am especially grateful to Juan Maldacena for discussions, detailed comments on the draft, and encouragement. I am supported by the Simons foundation through the It from Qubit Collaboration.

A Geodesic distance

We write the BTZ metric as

$$\begin{aligned} ds^2 &= -f(r)dt^2 + \frac{dr^2}{f(r)} + r^2 d\phi^2 \\ &= -\frac{4l^2 dudv}{(1+uv)^2} + r_h^2 \frac{(1-uv)^2}{(1+uv)^2} d\phi^2 \end{aligned}$$

where $f(r) = \frac{r^2 - r_h^2}{l^2}$. u, v are Kruskal coordinates. $\frac{r}{r_h} = \frac{1-uv}{1+uv}$.

Following [15], we compute the geodesic distance in BTZ geometry in embedding coordinates.

$$\cosh \frac{d}{l} = T_1 T_1' + T_2 T_2' - X_1 X_1' - X_2 X_2'$$

where

$$\begin{aligned} T_1 &= \frac{v+u}{1+uv}, & T_2 &= \frac{1-uv}{1+uv} \cosh \frac{r_h \phi}{l} \\ X_1 &= \frac{v-u}{1+uv}, & X_2 &= \frac{1-uv}{1+uv} \sinh \frac{r_h \phi}{l} \end{aligned}$$

A.1 Geodesic distance 1

Alice throws in a perturbation from left side at time t_w . When t_w is early enough, the geometry was given in [16][15]. There is a shockwave lying close to the horizon $u = 0$. Across the shockwave there is a shift in another Kruskal coordinates $v \rightarrow v + \alpha$ where $\alpha = \frac{\delta S}{2S} e^{-\frac{2\pi}{\beta} t_w}$, where S is the black hole entropy and δS is the increase of the entropy from the perturbation.

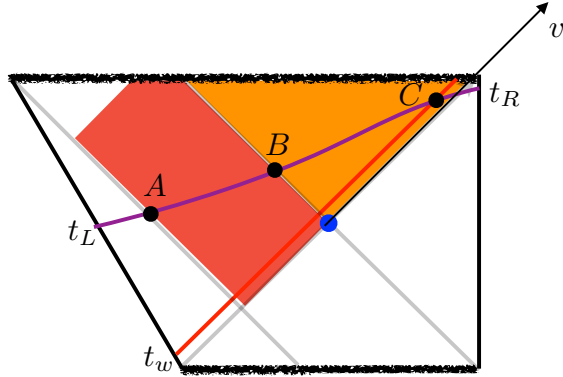


Figure 26: Geodesic length as a function of left time.

We calculate the geodesic length and volume of maximal surface inside and outside Bob's entanglement wedge.

After extremizing the geodesic length between two boundary points anchored at t_L and t_R , we get the Kruskal coordinates of the three intermediate points (Figure 26) when we

take $t_R \rightarrow \infty$:

$$\begin{aligned} A : (u, v) &= \left(\frac{1}{2} e^{\frac{r_h}{l^2} t_L}, 0 \right) \\ B : (u, v) &= \left(\frac{1}{2e^{-\frac{r_h}{l^2} t_L} + \alpha}, \alpha \right) \\ C : (u, v) &= \left(0, \frac{1}{2} \left(e^{\frac{r_h}{l^2} t_R} + e^{-\frac{r_h}{l^2} t_L} - \alpha \right) \right) \end{aligned}$$

We get

$$\begin{aligned} \frac{d_{AB}}{l} &= \log(1 + \alpha e^{t_L}) = \log\left(1 + e^{\frac{2\pi}{\beta}(t_L - t_w - t_*)}\right) \\ \frac{d_{BC}}{l} &= \frac{2\pi}{\beta}(t_R + t_L) - \log\left(1 + e^{\frac{2\pi}{\beta}(t_L - t_w - t_*)}\right) \end{aligned}$$

A.2 Geodesic distance 2

In this section, we fix $t_L \rightarrow +\infty$ and see how length of the part of the geodesic in the orange region depends on the right boundary time.

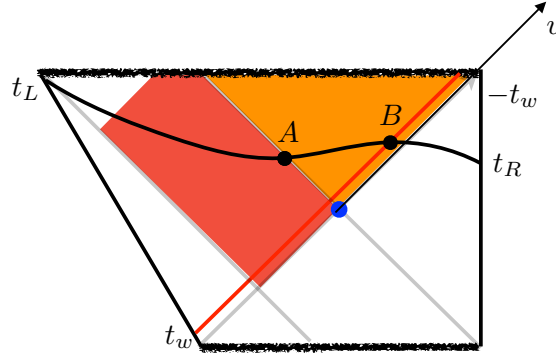


Figure 27: Geodesic length as a function of right time.

In Figure 27, The distance from the left boundary anchored at t_L to point B is given by

$$\begin{aligned} \frac{d_{LB}}{l} &= \log \frac{2R}{r_H} + \log \left(\frac{1 + e^{\frac{2\pi}{\beta}(t_R + t_L)} + \alpha e^{\frac{2\pi}{\beta} t_L}}{2} \right) \\ &\approx \log \frac{R}{r_h} + \frac{2\pi}{\beta}(t_R + t_L) + \log \left(1 + \alpha e^{-\frac{2\pi}{\beta} t_R} \right) \end{aligned}$$

The distance from the left boundary point to point A is given by

$$\frac{d_{LA}}{l} \approx \log \frac{2R}{r_h} + \log \left(1 + \alpha e^{\frac{r_h}{l^2} t_L} \right)$$

Taking the difference of these two, we get

$$\frac{d_{AB}}{l} \approx \frac{2\pi}{\beta} (t_R + t_w + t_*) + \log \left(1 + \alpha e^{-\frac{2\pi}{\beta} t_R} \right)$$

This is non zero when $t_R > -t_w - t_*$.

References

- [1] Juan Martin Maldacena, “Eternal black holes in anti-de Sitter,” *JHEP* **04**, 021 (2003), [arXiv:hep-th/0106112 \[hep-th\]](#)
- [2] Juan Maldacena and Leonard Susskind, “Cool horizons for entangled black holes,” *Fortsch. Phys.* **61**, 781–811 (2013), [arXiv:1306.0533 \[hep-th\]](#)
- [3] Brian Swingle, “Entanglement Renormalization and Holography,” *Phys. Rev.* **D86**, 065007 (2012), [arXiv:0905.1317 \[cond-mat.str-el\]](#)
- [4] Thomas Hartman and Juan Maldacena, “Time Evolution of Entanglement Entropy from Black Hole Interiors,” *JHEP* **05**, 014 (2013), [arXiv:1303.1080 \[hep-th\]](#)
- [5] Leonard Susskind, “Entanglement is not enough,” *Fortsch. Phys.* **64**, 49–71 (2016), [arXiv:1411.0690 \[hep-th\]](#)
- [6] Douglas Stanford and Leonard Susskind, “Complexity and Shock Wave Geometries,” *Phys. Rev.* **D90**, 126007 (2014), [arXiv:1406.2678 \[hep-th\]](#)
- [7] Daniel A. Roberts, Douglas Stanford, and Leonard Susskind, “Localized shocks,” *JHEP* **03**, 051 (2015), [arXiv:1409.8180 \[hep-th\]](#)
- [8] Adam R. Brown, Daniel A. Roberts, Leonard Susskind, Brian Swingle, and Ying Zhao, “Holographic Complexity Equals Bulk Action?,” *Phys. Rev. Lett.* **116**, 191301 (2016), [arXiv:1509.07876 \[hep-th\]](#)
- [9] Ying Zhao, “Uncomplexity and Black Hole Geometry,” *Phys. Rev. D* **97**, 126007 (2018), [arXiv:1711.03125 \[hep-th\]](#)

- [10] Patrick Hayden and John Preskill, “Black holes as mirrors: Quantum information in random subsystems,” *JHEP* **09**, 120 (2007), [arXiv:0708.4025 \[hep-th\]](#)
- [11] Leonard Susskind and Ying Zhao, “Switchbacks and the Bridge to Nowhere,” (2014), [arXiv:1408.2823 \[hep-th\]](#)
- [12] Leonard Susskind, Larus Thorlacius, and John Uglum, “The Stretched horizon and black hole complementarity,” *Phys. Rev. D* **48**, 3743–3761 (1993), [arXiv:hep-th/9306069](#)
- [13] Tevian Dray and Gerard ’t Hooft, “The Effect of Spherical Shells of Matter on the Schwarzschild Black Hole,” *Commun. Math. Phys.* **99**, 613–625 (1985)
- [14] Stephen H. Shenker and Douglas Stanford, “Multiple Shocks,” *JHEP* **12**, 046 (2014), [arXiv:1312.3296 \[hep-th\]](#)
- [15] Stephen H. Shenker and Douglas Stanford, “Black holes and the butterfly effect,” *JHEP* **03**, 067 (2014), [arXiv:1306.0622 \[hep-th\]](#)
- [16] Tevian Dray and Gerard ’t Hooft, “The Gravitational Shock Wave of a Massless Particle,” *Nucl. Phys.* **B253**, 173–188 (1985)